Organic & Biomolecular Chemistry

PAPER

View Article Online
View Journal | View Issue

Published on 08 November 2019. Downloaded by University of Texas Libraries on 1/4/2020 5:05:00 AM.

Check for updates

Cite this: *Org. Biomol. Chem.*, 2019, **17**, 10052

(3*S*,4*R*)-3,4-Dihydroxy-*N*-alkyl-L-homoprolines: synthesis and computational mechanistic studies†

David S. Freitas, ‡[a] Cristina E. A. Sousa, ‡[a] Joana Parente,[a] Artem Drogalin,[a] António Gil Fortes,[a] Nuno M. F. S. A. Cerqueira *[b] and Maria J. Alves *[a]

Received 3rd October 2019,
Accepted 5th November 2019

DOI: 10.1039/c9ob02141h

rsc.li/obc

This is the first synthetic report of (3*S*,4*R*)-dihydroxy-*N*-alkyl-L-homoprolines described so far. 2,4-*O*-Benzylidene-D-erythrose was obtained from D-glucose with an improved yield, and then transformed into the title (3*S*,4*R*)-dihydroxy-*N*-alkyl-L-homoprolines, in a two-step strategy, with excellent overall yields. Hydrogenolysis of the benzyl group led to the *N*H congener. The synthesis of final products from 1,4-lactone intermediates was studied by computational means either under acidic or basic conditions. The theoretical mechanism studies fully explain the experimental results: (a) an equilibrium between L-homoprolines and their bicyclic counterparts is established in acids; (b) the equilibrium suffers a complete displacement towards the L-homoproline side in a basic medium.

1. Introduction

Carbohydrates have served as chiral starting materials for the synthesis of several amino acids.[1–3] Some of these syntheses are multi-stage, involving considerable manipulation of protecting groups. However, some elegant protocols are known for 3,4-dihydroxyprolines.[4] Three members of the L-series have been isolated from natural sources: **1**, from *Navicula pelliculosa;*[5] **2** from *Amanita virosa;*[6] and **3**, the sixth residue of the decapeptide sequence of Mefp1 (Fig. 1), an adhesive protein, from the marine mussel *Mytilus edulis.*[7] Though, the syntheses of homoproline congeners are very scarce, only two methods have been published for these compounds: one, by the Davis group,[8] and another from our laboratory.[9] This is, as far as we know, the first report for the synthesis of L-3,4-dihydroxyprolines. A major feature of proline amino acids in Nature is related to the rigidity imposed into the peptide sequence in which proline is incorporated, leading to protein folding (α-,β-,γ-turns), which is known to play important roles in: (i) the tertiary structure of proteins, (ii) molecular/cellular recognition processes, and (iii) interactions between substrates and receptors.[10–14] However, in the modified peptide backbones the conformational torsions have been successfully attained through the introduction of amino acids other than L-proline; β,γ-amino acids, amino acids of the D-series, and various types of cyclic monomers.[10,15] β-Amino acids are the best-studied among those compounds.[16,17] In this context, the development of asymmetric synthetic routes for the synthesis of homoprolyl residues is highly desirable as new templates in the design of specific turn-mimics of biologically active molecules. The present work intends to be a contribution to the required pool of homoproline molecules. Besides, the two hydroxyl groups at 3,4-positions of the proline ring being polar and capable of hydrogen-bonding can be easily tunable into nonpolar groups, *e.g.* by acetal protection. Additional importance of these compounds comes from the recent synthesis of their D-congeners, obtained by a divergent synthesis from 2,4-*O*-benzilidene-D-erythrose.[9] Knowing that a matching configuration of amino acids is crucial in shaping the outcome for the peptide secondary structure,[15] the choice between D- and L-structures is preeminent in the design of new peptide foldamers.

2,4-*O*-Benzilidene-D-erythrosylimines generated *in situ* from D-erythrose display a complete facial selectivity towards 1-(*tert*-butyldimethylsilyloxy)-1-methoxyethene nucleophilic addition giving the *R* configuration at the new stereogenic centre. The acid treatment of adducts followed by basic treatment triggers

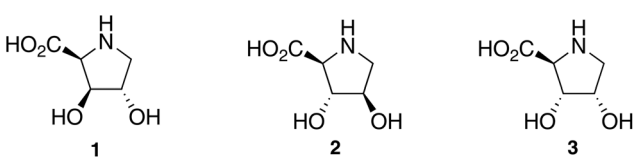

Fig. 1 Dihydroxyprolines isolated from natural sources.

[a]*Departamento de Química, Universidade do Minho, Campus de Gualtar, 4710-057 Braga, Portugal. E-mail: mja@quimica.uminho.pt*
[b]*UCIBIO@REQUIMTE, Departamento de Biomedicina da Faculdade de Medicina da Universidade do Porto, Alameda Professor Hernâni Monteiro, 4200-319 Porto, Portugal. E-mail: nunoscerqueira@med.up.pt*

†Electronic supplementary information (ESI) available. See DOI: 10.1039/c9ob02141h

‡The first authors.

This journal is © The Royal Society of Chemistry 2019

Published on 08 November 2019. Downloaded by University of Texas Libraries on 1/4/2020 5:05:00 AM.

a reaction cascade leading to an L-homoproline in excellent overall yields. The computational results are consistent with the formation of (3*S*,4*R*)-dihydroxy L-homoprolines in two stages from the imine adducts.

2. Experimental results and discussion

2,4-*O*-Benzylidene-D-erythrose[18] (**4**) is obtained on a 10 g scale from D-glucose, by adapting a known procedure for the synthesis of 2,4-*O*-isopropylidene-D-erythrose.[19] 2,4-*O*-Benzylidene-D-erythrose reacted with alkyl amines, as they did with aromatic amines before[20] to give the respective *N*-alkylimines **5**. Imines **5** were found to be excellent chiral templates able to induce complete stereoselectivity in nucleophilic additions with 1-(*tert*-butyldimethylsilyloxy)-1-methoxyethene, furnishing single adducts **6a–d**, in high yields (Scheme 1). Compounds **6a–d** were purified by flash column chromatography in silica. It was found that silica promotes cyclization to six-membered lactones **7a–d** during the course of chromatographic purification. The ^{1}H NMR spectra of adducts **6a–d** showed the presence of lactones **7a–d** as contaminants. In case **a**, an enriched sample of **7a** was obtained during chromatography.

In a previous work, the acid treatment of either compound **9** or **10** led to 1,4-lactone **11**. Scheme 2 shows how the spatial proximity between the attacking oxygen (O-1) and the carbonyl can easily lead to 1,4-lactone **11** in both cases. Computational mechanistic studies were developed for some of these cases.[21]

Accordingly, compounds **6a–d** (together with their contaminants **7a–d**) were subjected to strong acid conditions with the aim to generate lactones **12a–d** (Scheme 3).

It is likely that the matching configuration of the amino group and the 1,2-dihydroxyethyl arm in lactone **12** makes the aminocyclization a much easier process than the aminocyclization of its epimer **11**.[9] Lactone **11** had to undergo bromination at the primary hydroxyl group in order to make cyclization occur. Theoretical calculations have confirmed that compound **12a** can be converted into **13a** under other acids besides HBr (HCl, TFA, see the third section) by a relatively easy process.

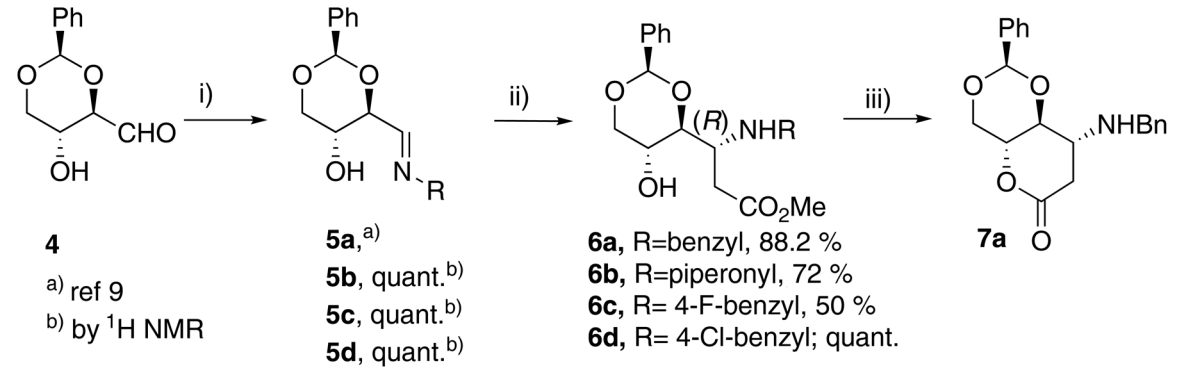

Scheme 1 Synthesis of D-erythrosyl alkylimines **5** and its reactions with 1-(*tert*-butyldimethylsilyloxy)-1-methoxyethene – (i) alkylamines 0.7 equiv., THF (dry), 1 h, 35 °C, 4 Å MS, N_2 (g); (ii) $BF_3{\cdot}OEt_2$ 0.7 equiv., 1-(*tert*-butyldimethylsilyloxy)-1-methoxyethene 0.7 equiv., THF (dry), 4 Å MS, N_2 (g), −84 °C to rt, 2 h; (iii) ethyl acetate : pet. ether (1 : 1), r.t., prolonging contact with silica (in a chromatographic column).

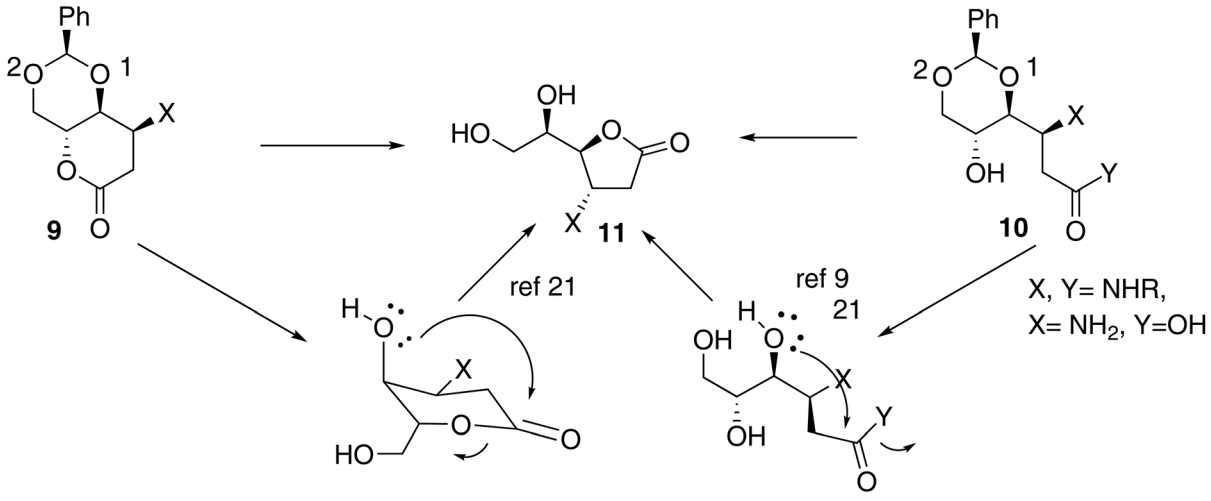

Scheme 2 Synthesis of 1,4-lactone **11** obtained by the acid treatment of D-erythrose 6-carbon chain derivatives **9** and **10**.

Published on 08 November 2019. Downloaded by University of Texas Libraries on 1/4/2020 5:05:00 AM.

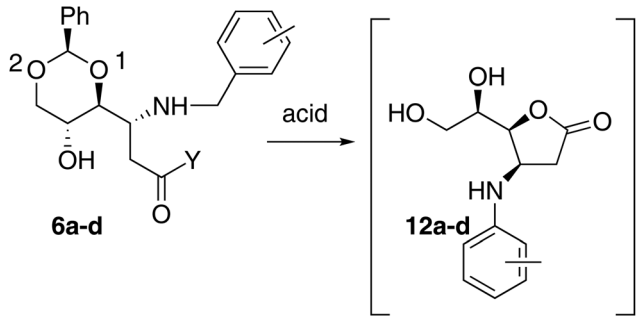

Scheme 3 Synthesis of lactones **12a–d** obtained by the acid treatment of compounds **6a–d**.

The treatment of compound **6a** with TFA led to an evanescent compound, tentatively assigned as compound **12a**. It was observed over the reaction period in aliquots studied by ^{1}H NMR. After a 5 h reaction course at room temperature, this compound was the main species in the reaction mixture. Over the time (5–8 days), a dynamic equilibrium had been reached leading to a 1 : 3 : 1 mixture of three components: **13a** (major) together with **8a** and **12a** (Scheme 4). Any attempt to isolate compound **12a** by chromatography was found to be not possible; the mixture systematically evolves to compounds **13** and **8**. The obtained products were found to be in a 2 (**13a**) : 1 (**8a**) ratio in reactions run in standard HCl–dioxane, a 1 : 1 mixture with HBr in acetic acid, and a 3 (**13a**) : 1 (**8a**) with 6 M trifluoroacetic acid in dioxane. In the last case, the ratio did not change by prolonging the reaction time for a week. The full conversion of the bicyclic compounds **13** into L-homoprolines **8** occurs by the basification of the reaction medium with KOH or triethylamine followed by acidic resin treatment, to adjust the pH to 7. In some spectra of homoprolines **8**, vestigial amounts of the respective bicyclic compounds are always present. Compounds **8a–d** are generally formed in high yields. The debenzylation of homoproline **8a** was achieved by hydrogenation in the presence of Pd/C at room temperature (Scheme 4).

When a D_2O solution of the obtained compound **8a** contained in a NMR tube was treated with TFA-d_8 **8a** it was found that an equilibrium between **8a** and **13a** is re-established. Computational mechanistic studies clearly show how energetics favors the equilibrium back in the acidic medium.

3. Computational studies

Computational studies were carried out, using density functional theory, to understand the mechanism of the reactions involving the reaction of 1,4-lactones **12a** under different acidic conditions, eventually followed by basic conditions, and from which the *N*-benzyl (3*S*,4*R*)-dihydroxy L-homoproline **8a** is obtained.

The computational results have shown that although the reaction is done experimentally in one-pot synthesis, the mechanism goes through several sequential stages and involves the formation of the intermediate **13a**, as described in the next sections.

3.1. Stage 1: formation of the reaction intermediate 13a from 1,4-lactone 12a

An intramolecular cyclisation of lactone **12a** occurs under acidic conditions at the first stage (Fig. 2). In compound **12a**, nitrogen N1 and carbon C2 are at a 3.13 Å distance from each other in the reactants. The proton from HCl is stabilized by a hydrogen bond network provided by one water molecule W1 and the hydroxyl group (O2) of the lactone.

The transition state of the reaction is characterized by an imaginary frequency at 386.33i cm^{-1}. This stationary point reveals that nitrogen N1 and carbon C2 become closer to each other (2.26 Å) at the same time that the bond lengths between carbon C2 and oxygen O2 become extended (1.87 Å *versus* 1.44 Å in the

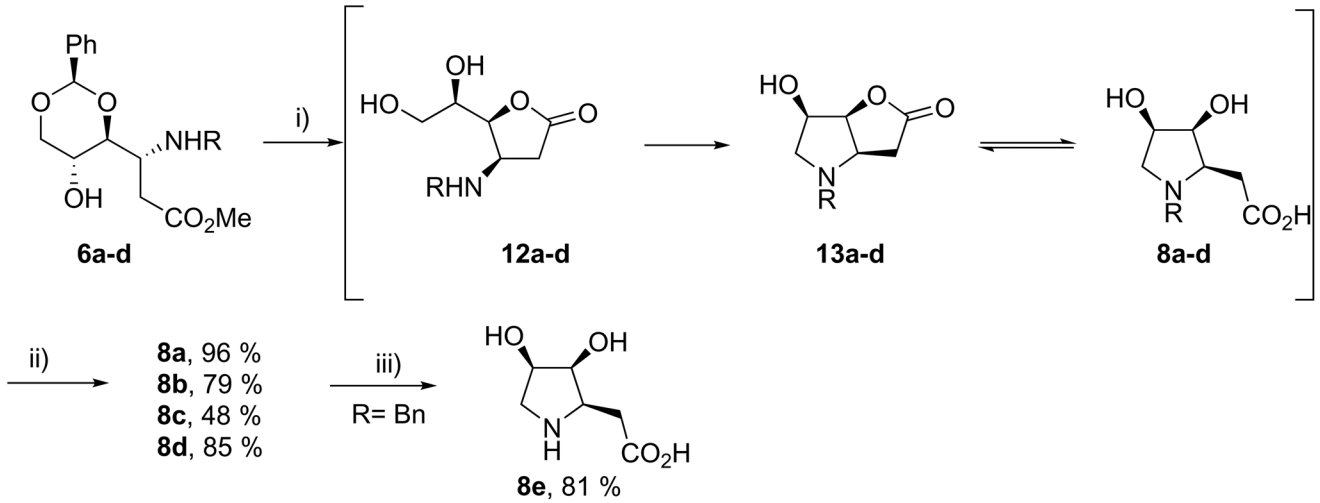

Scheme 4 Synthesis of L-homoprolines **8a–d** – (i) HCl 6 M, dioxane : water 1 : 1, rt, 2 h; (ii) (a) KOH 6 M; rt, overnight; (b) Amberlite IR-120 (H^+), pH 7, rt; (iii) (a) Pd/C, 10 mol%, H_2, 1 atm, MeOH, 1,1,2-trichloroethane (1.1 equiv.), 2 days; (b) KOH (0.01 M) until pH 12.

 This journal is © The Royal Society of Chemistry 2019

Published on 08 November 2019. Downloaded by University of Texas Libraries on 1/4/2020 5:05:00 AM.

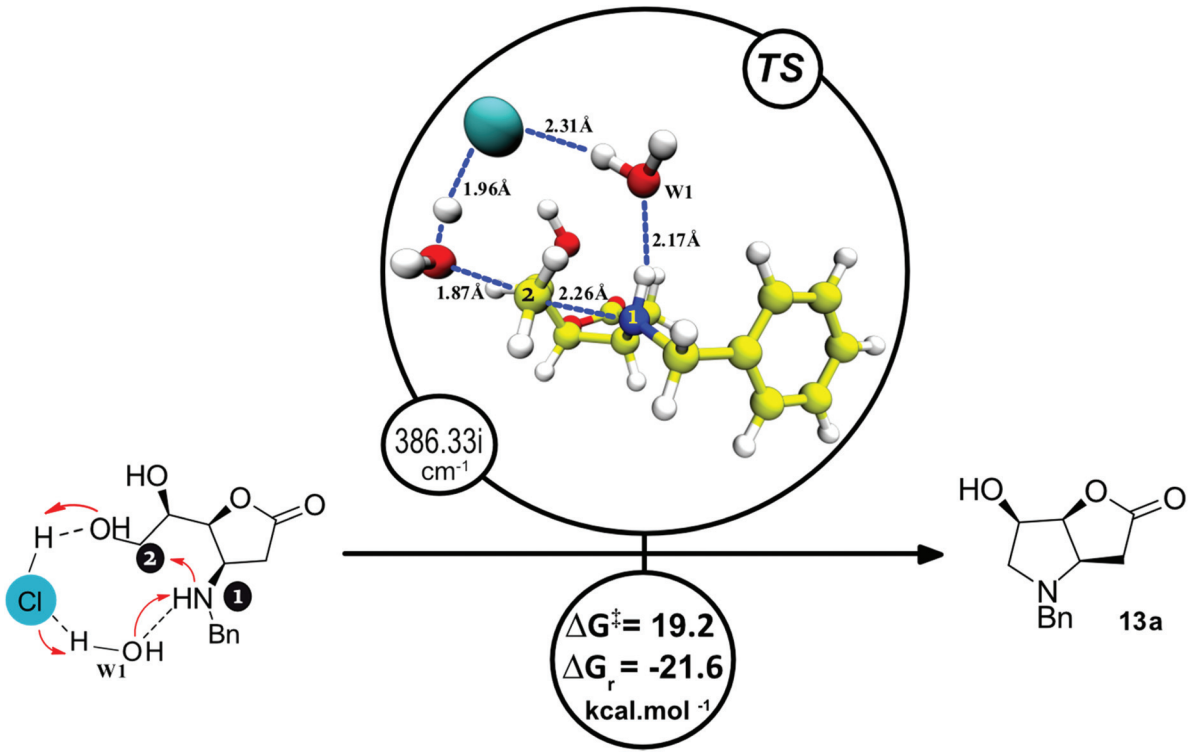

Fig. 2 Aminocyclization mechanism for the synthesis of bicyclic compound **13a** from **12a**.

reactants), enabling the simultaneous proton transfer among them, through the HCl molecule and the water molecule W1.

At the end of this stage, the intra-molecular cyclisation is complete. Carbon C2 and nitrogen N1 become covalently bonded to each other by a single bond (1.52 Å *versus* 3.13 Å in the reactants). At the same time, one proton migrates from nitrogen N1 to the water molecule W1 and from the latter one to oxygen O2 of the lactone, through HCl. This process results in the cleavage of the bond between oxygen O2 and carbon C2 (3.17 Å *versus* 1.44 Å in the reactants) and the formation of one water molecule (W2).

This reaction requires a free activation energy of 19.2 kcal mol^{-1} and is exergonic with −21.6 kcal mol^{-1}.

The intra-molecular network of hydrogen bonds plays an important role in this step since: (i) it enables the correct alignment of nitrogen N1 and carbon C2 within the lactone, making them ready for the nucleophilic attack, and (ii) it enables the proton transfer from nitrogen N1 to the hydroxyl group bonded to carbon C2, through the HCl molecule. The HCl molecule behaves as a catalyst in the reaction facilitating the proton transfer through the water molecules that is determinant for the cyclisation process.

Experimentally, compound **12**, once formed, easily evolves to **13**. The computational results showed a free activation energy ($\Delta G^{\ddagger}$ = 19.2 kcal mol^{-1}) compatible with the reaction's room temperature. As this conversion is very exergonic (ΔG_r = −21.6 kcal mol^{-1}) the reverse step is not possible, which is in accordance with experimental results.

3.2. Stage 2: formation of L-homoproline 8a from bicyclic compound 13a

The next stage of the mechanism involves the formation of the homoproline **8a** from the intermediate **13a**, obtained in the end of the first stage. Experimentally, this reaction was found to diverge whenever acidic or basic conditions were employed. Under acidic conditions, an equilibrium is observed between compounds **13a** and **8a**. However, the yields of the reactions change significantly depending on the type of acid that is employed (HCl, HBr and TFA). Under basic conditions, the reaction is very efficient, giving solely compound **8a**.

The computational results explain the mechanistic differences, both under acid and basic conditions as described in detail below.

3.2.1. Acid catalysis. Under acid conditions, the reaction involves the cleavage of the lactone ring in intermediate **13a**. The reaction requires the direct participation of one water molecule and an acid species molecule, and it is completed in two sequential steps (Fig. 3). The mechanism is very similar for the different acids that were employed (HCl, HBr or TFA).

In the first step, the adduct formation occurs. The proton from the acid species approaches the oxygen O1 of the reactant and establishes one hydrogen bond with it (in average 1.68 Å), and a weaker interaction with the neighbouring water molecule (in average 2.43 Å).

The transition states of these additions are characterized by one imaginary frequency (see the first step in Fig. 3). The bond

Published on 08 November 2019. Downloaded by University of Texas Libraries on 1/4/2020 5:05:00 AM.

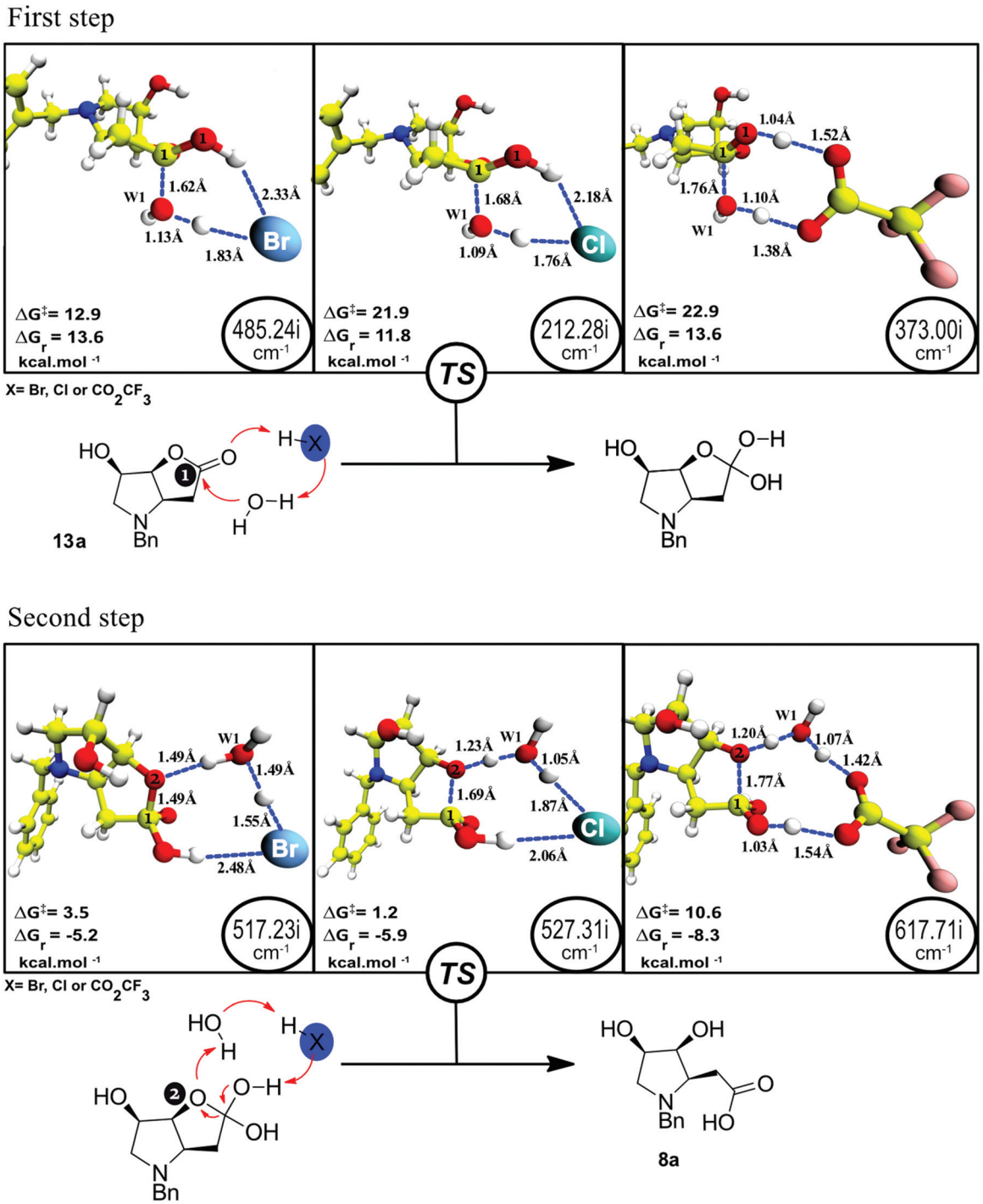

Fig. 3 Mechanism involved in lactone cleavage in compound **13a** to form compound **8a** under HCl, HBr and TFA.

length between carbon C1 and oxygen O1 increases to around 1.33 Å (1.22 Å in the reactants), at the same time the oxygen from the water molecule (W1) becomes aligned with carbon C1 and very close to it (in average 1.69 Å *versus* 3.30 Å in the reactants), and the acid proton establishes a bond with oxygen O1.

The adduct is formed when the carbon C1–oxygen O1 bond is 1.38 Å (*versus* 1.22 Å in compound **13a**), and the hydroxyl group from the water molecule becomes covalently bonded to carbon C1 (around 1.44 Å). At the same time, the proton from the water molecule migrates to the acid.

The free activation energy of the first step is lower when HBr is used and higher when TFA and HCl are employed (Table 1). No significant differences are observed in the free reaction energy. In all the studied cases, the reactions are endergonic and with similar values.

 This journal is © The Royal Society of Chemistry 2019

Published on 08 November 2019. Downloaded by University of Texas Libraries on 1/4/2020 5:05:00 AM.

The second step involves the ring cleavage with the formation of compound **8a**.

In the adduct, carbon C1 and oxygen O2 are bonded to each other by a covalent bond (1.50 Å in HBr and HCl, 1.47 Å in TFA) and the proton from the acid species is bonded to a water molecule W1 (1.07 Å, except for TFA (1.54 Å)).

The transition states of the second step are characterized by one imaginary frequency (see the second step in Fig. 3). The bond between carbon C1 and oxygen O2 starts to elongate (in average 1.65 Å), and one hydrogen molecule from the water molecule W1 becomes very closer to oxygen O2 (in average 1.31 Å *versus* 1.53 Å in HBr and HCl, and 1.78 Å in TFA in the adducts).

In the product, the bond between carbon C1 and oxygen O2 is cleaved (2.45 Å in HBr/HCl, 2.72 Å in TFA), and the protic acid is on the way to be regenerated from the hydroxyl group converted into carbonyl.

Overall, the addition–elimination reaction mechanisms do not show significant differences within the acids employed (HBr, HCl and TFA). The calculated free energies show that the first step is the rate-limiting one in all studied reactions. The reaction with the best full energetic profile (faster kinetics) is the one where HBr is employed. This happens due to the largest atomic radius of bromine that makes the proton shuttle more efficiently in HBr, especially in the first step (see Fig. 3). The slowest reaction is the one where TFA is employed, due to the heist activation free energies that are observed in both steps (Table 1).

The energetic profile of the theoretical calculations of hydrolysis in HBr in acetic acid showed a free activation energy of 12.9 kcal mol^{-1} in the first step, and 3.5 kcal mol^{-1} in the second step. As so, an open equilibrium with very low free activation energies in both sides should operate. The ratio between compounds **13a**/**8a** is nevertheless difficult to predict from the differences in activation and reaction energies.

The energetic profile of the theoretical calculations of hydrolysis in HCl showed that the first step ($\Delta^{\ddagger}$ = 21.9 kcal mol^{-1}) controls the lactone hydrolysis process. At room temperature the energetic barrier is predicted to be surpassed, counting with an energy supplement released in the formation of compound **13a**. The second step showed a very low free activation energy ($\Delta^{\ddagger}$ = 1.3 kcal mol^{-1}), and it is exergonic (Δ_r = −5.9 kcal mol^{-1}). Being so, the reversal process needs only 16 kcal mol^{-1} to be surmounted. These findings go in line with the experimental equilibrium observed in the hydrolysis of the bicyclic lactone **13a** with HCl. The intermediate **13a** evolved to compound **8a** in equilibrium with **13a** in 2 (**13a**) : 1 (**8a**).

In a separated experiment, it was found that compound **8a** quickly sets an equilibrium back with **13a**. The experiment consisted of adding TFA-d_8 to a solution of **8a** in D_2O contained in a NMR tube. After 30 minutes, a 3 (**13a**) : 1 (**8a**) ratio was verified.

The energetic profile obtained from the theoretical calculations for this transformation is only 18 kcal mol^{-1} for the limiting step, which is likely to take place at room temperature. From the thermodynamic point of view compound **13** is favored over **8a** in *ca.* 5 kcal mol^{-1}. Interestingly, the intermediate adduct for the direct/inverse processes requires similar free activation energies for both sides of the reaction (direct: 10.6 kcal mol^{-1}; inverse: 9.3 kcal mol^{-1}). The reaction point of equilibrium was found to be dependent on the ground energy of **8a** and **13a**.

3.2.2. Basic catalysis. Under basic conditions, only one product is obtained in the end of the reaction, compounds **8a–d**. The mechanism requires the presence of a base, KOH, and two water molecules. The reactions are complete in two sequential steps (Fig. 4).

The computational results have shown that the reaction requires two steps; the first step involves the formation of a zwitterionic reaction intermediate.

In the reagent, compound **13a**, the bond length between carbon C1 and the oxygen O of KOH is 3.05 Å. Its position is stabilized by two water molecules that are aligned with oxygen O2, through a network of hydrogen bonds (2.65 Å and 1.89 Å).

The transition state of this reaction is characterized by one imaginary frequency at 78.47i cm^{-1}. In these structures, the central role played by the potassium cation on the reaction becomes clear. It favours: (i) the alignment of the hydroxide with carbon C1 (2.55 Å), (ii) the hydrogen bond between water molecule 2 (W2) and the carbonyl group (1.81 Å) and, (iii) the hydrogen bond between water molecule 2 (W2) with the potassium (2.81 Å).

In the end of this reaction, a stable zwitterionic reaction intermediate is obtained. Carbon C1 acquires a tetrahedral configuration, and oxygen O1 becomes negatively charged (−1.00 a.u. *versus* −0.78 a.u. in the reactants). The negative charge is stabilized by one water molecule, W2, that is now very close to the positively charge potassium. The water molecule W1 is also close to the potassium cation, but also interacts with oxygen O2 through a short hydrogen bond (1.99 Å).

This reaction is almost spontaneous requiring a very low free activation energy (1.9 kcal mol^{-1}) and it is exergonic with −9.4 kcal mol^{-1}.

The second step involves the cleavage of the zwitterionic intermediate into compound **8a**.

The reactant of this step is very similar to the product of the last step. Carbon C1 is firmly attached to oxygen O2 by a covalent bond (1.59 Å) and the potassium cation (0.94 a.u.) continues to be stabilized by the oxygen atoms provided by the two water molecules and the hydroxyl group that is now attached to carbon C1.

Table 1 Activation free energies ($\Delta^{\ddagger}$) and reaction free energies (Δ_r) for the transformation of compound **13a** into **8a** in TFA, HCl, and HBr

	First step		Second step		
	$\Delta^{\ddagger}$ (kcal mol^{-1})	Δ_r (kcal mol^{-1})	$\Delta^{\ddagger}$ (kcal mol^{-1})	Δ_r (kcal mol^{-1})	**13a**/**8a**
TFA	22.9	13.6	10.6	−8.3	3 : 1
HCl	21.9	11.8	1.2	−5.9	2 : 1
HBr	12.9	13.6	3.5	−5.2	1 : 1

Published on 08 November 2019. Downloaded by University of Texas Libraries on 1/4/2020 5:05:00 AM.

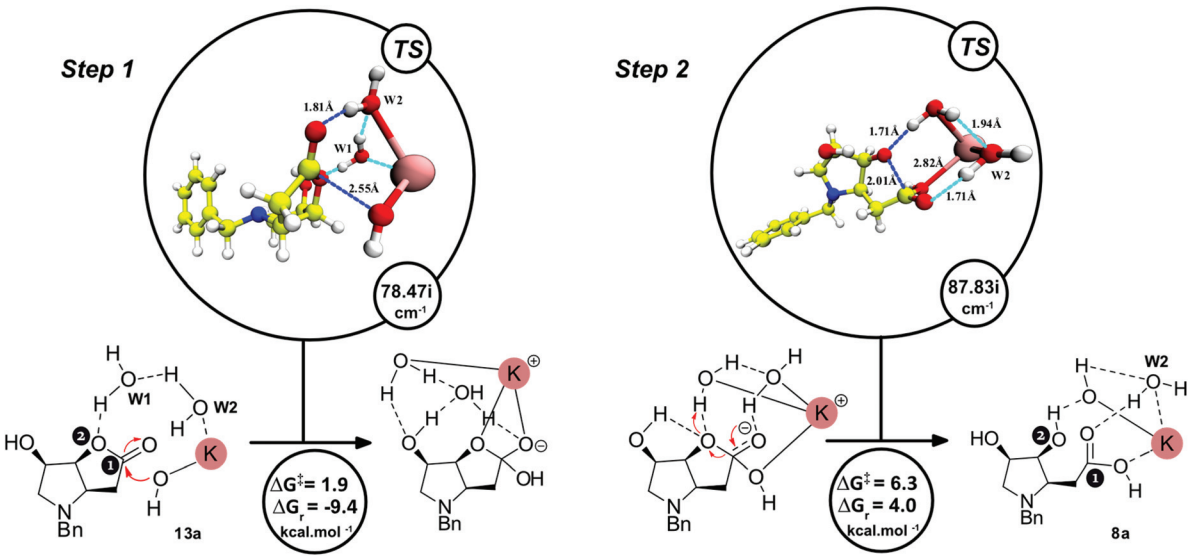

Fig. 4 Mechanism involved in lactone unit cleavage in compound **13a** to form compound **8a** under basic conditions.

The transition state of the studied reaction is characterized by one imaginary frequency at 87.83i cm^{-1}. The bond length between carbon C1 and oxygen O2 starts to elongate (2.01 Å *versus* 1.59 Å in the reactant) and one of the hydrogens from water molecule W1 becomes very close to oxygen O2.

In the product of this reaction, the formation of compound **8a** is complete. The bond between carbon C1 and oxygen O2 is cleaved (2.41 Å *versus* 1.59 Å in the reactant), and KOH is regenerated after the proton transfer from water molecule W2 to water molecule W1.

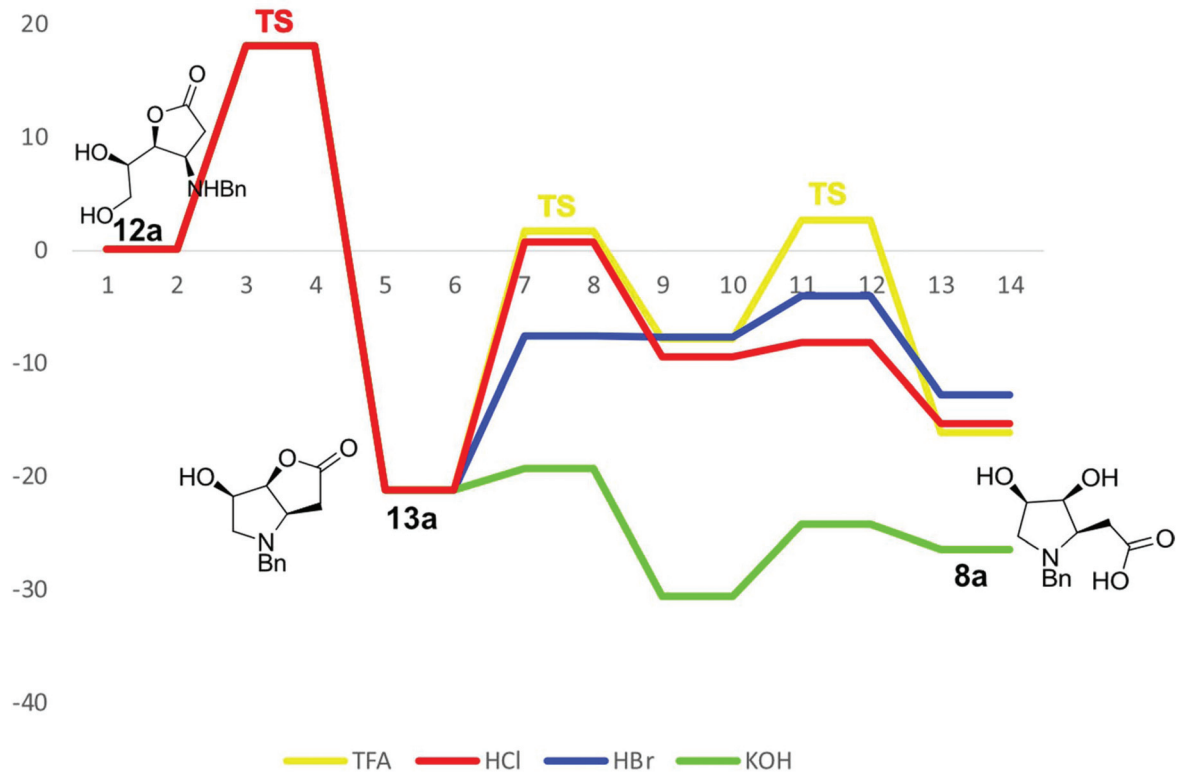

Fig. 5 Energetic profile of all the studied reactions to yield the formation of *N*-benzyl-(3*S*,4*R*)-dihydroxy L-homoprolines **8a** under acidic and basic conditions.

This journal is © The Royal Society of Chemistry 2019

Published on 08 November 2019. Downloaded by University of Texas Libraries on 1/4/2020 5:05:00 AM.

Similar to the previous step, this reaction requires a low free activation energy (6.3 kcal mol^{-1}), being slightly endergonic with 4.0 kcal mol^{-1}.

From the experimental work, it is known that the equilibrium is completely shifted towards to the right giving **8a**. This is in accordance with the theoretical results obtained which display an energetically favoured profile (Fig. 5).

4. Experimental

4.1. General

All reagents were purchased from Sigma-Aldrich, Acros, TCI or Alfa Aesar and used without further purification, except for *p*-toluenesulfonic acid monohydrate which was dried under a vacuum pistol at 120 °C, THF was dried by reflux under Na(s), and $BF_3{\cdot}OEt_2$ by distillation. Aldehyde **4** [18,19] and imine **6a** [9] were synthesized following the procedures described in the literature. An optimized synthesis of **4** was obtained from a synthetic description of an analog described in the literature.[19]

4.2. Optimized synthesis of 2,4-benzylidene-D-erythrose

(i) Acetal protection of D-glucose to yield (2*R*,4a*R*,6*S*,7*S*,8*S*,8a*S*)-2-phenylhexahydropyrano[3,2-*d*][1,3]dioxine-6,7,8-triol.[18]

(ii) To a solution of $NaIO_4$ (8.2 g; 0.038 mol; 2.2 equiv.) in water (62 mL), refrigerated at 0 °C, and kept at pH = 4, was added dropwise a suspension of (2*R*,4a*R*,6*S*,7*S*,8*S*,8a*S*)-2-phenylhexahydropyrano[3,2-*d*][1,3]dioxine-6,7,8-triol (5 g), in water (21 mL), with permanent pH control (pH ≥ 4), by the addition of aqueous sodium hydroxide 8 M (~8 mL). The temperature was kept under 10 °C until total dissolution (~3 h). After the 3 h reaction time, the pH was adjusted to 6.5, and the stirring was continued for another 2 h, at room temperature. The solution was evaporated and the residue was dried under vacuum. Ethyl acetate (40 mL) is added to the residue and the flask was heated for 2 min at 80 °C under stirring. The suspension formed was filtered and the solid residue was washed with ethyl acetate (3 × 30 mL). The combined liquid fractions were dried over anhydrous sodium sulphate for 1 h, and concentrated in the rotary evaporator to yield 3.69 g (95%) of 2,4-*O*-benzylidene D-erythrose.[18,19]

4.3. Synthesis of D-erythrosyl benzylimine 5a–c

4.3.1. General procedure. To a solution of aldehyde **4** (150–200 mg; 0.72–0.96 mmol) in dry THF (4–10 mL), containing activated 4 Å molecular sieves (1.0 g), was added the amine (57–84 μL; 63–110 mg; 0.50–0.67 mmol) under magnetic stirring and an N_2 atmosphere. The reaction mixture was kept stirring for 1 h at 35 °C. According to the ^{1}H NMR, products are clear yellow oils, virtually pure, and used in the next step without purification.

4.3.2. Synthesis of (2*R*,4*S*,5*R*)-4-((*E*)-(benzylimino)methyl)-2-phenyl-1,3-dioxan-5-ol (5a). Aldehyde **4** (150 mg, 0.72 mmol); THF (4 mL); benzylamine (55 μL, 54 mg, 0.50 mmol).

^{1}H NMR (400 MHz, $CDCl_3$) δ 3.73 (t, J = 10.8 Hz, 1H, *H*-6), 4.04 (ddd, J = 10.4, 8.8, 5.2 Hz, 1H, *H*-5), 4.22 (dd, J = 8.8, 1.6 Hz, 1H, *H*-4), 4.38 (dd, J = 10.8, 5.2 Hz, 1H, *H*-6), 4.77 (s, 2H, *H*-1″), 5.69 (s, 1H, *H*-2), 7.36–7.65 (m, 10H, Ph–CH), 7.98 (d, J = 1.6 Hz, 1H, *H*-1′) ppm.

4.3.3. Synthesis of (2*R*,4*S*,5*R*)-4-((*E*)-((benzo[*d*][1,3]dioxol-4-ylmethyl)imino)methyl)-2-phenyl-1,3-dioxan-5-ol (5b). Aldehyde **4** (150 mg; 0.72 mmol); THF (5 mL); piperonylamine (63 μL; 76 mg; 0.50 mmol). ^{1}H NMR (400 MHz, $CDCl_3$) δ 3.73 (t, J = 10.4 Hz, 1H, *H*-6), 4.02 (ddd, J = 10.4, 8.8, 5.2 Hz, 1H, *H*-5), 4.20 (dd, J = 8.8, 1.6 Hz, 1H, *H*-4), 4.37 (dd, J = 11.2, 5.2 Hz, 1H, *H*-6), 4.55 (s, 2H, *H*-1″), 5.58 (s, 1H, *H*-2), 6.69–6.83 (m, 3H, *H*–Ph), 7.37–7.42 (m, 3H, *H*–Ph), 7.51–7.53 (m, 2H, *H*–Ph), 7.92 (d, J = 1.2 Hz, 1H, *H*-1′) ppm.

4.3.4. Synthesis of (2*R*,4*S*,5*R*)-4-((*E*)-((4-fluorobenzyl)imino)methyl)-2-phenyl-1,3-dioxan-5-ol (5c). Aldehyde **4** (150 mg, 0.72 mmol); THF (5 mL); 4-(fluoro)benzylamine (57 μL; 63 mg; 0.50 mmol). ^{1}H NMR (400 MHz, $CDCl_3$) δ 3.73 (t, J = 10.4 Hz, 1H, *H*-6), 4.03 (ddd, J = 10.4, 8.8, 5.2 Hz, 1H, *H*-5), 4.22 (dd, J = 8.8, 1.6 Hz, 1H, *H*-4), 4.49 (dd, J = 10.8, 5.2 Hz, 1H, *H*-6), 4.62 (s, 2H, *H*-1″), 5.59 (s, 1H, *H*-2), 7.04 (t, J = 8.8 Hz, 2H, *H*–Ph), 7.23 (dd, J = 5.2, 3.6 Hz, 2H, *H*–Ph), 7.35–7.42 (m, 3H, *H*–Ph), 7.52 (dd, J = 7.2, 2 Hz, 2H, *H*–Ph), 7.96 (d, J = 1.2 Hz, 1H, *H*-1′).

4.3.5. Synthesis of (2*R*,4*S*,5*R*)-4-((*E*)-((4-chlorobenzyl)imino)methyl)-2-phenyl-1,3-dioxan-5-ol (5d). Aldehyde **4** (200 mg, 0.96 mmol); THF (10 mL); 4-(chloro)benzylamine (82 μL, 95 mg, 0.67 mmol). ^{1}H NMR (400 MHz, $CDCl_3$) δ 3.72 (t, J = 10.4 Hz, 1H, *H*-6), 4.03 (ddd, J = 10, 8.8, 5.2 Hz, 1H, *H*-5), 4.22 (dd, J = 8.8, 1.2 Hz, 1H, *H*-4), 4.38 (dd, J = 10.8, 5.2 Hz, 1H, *H*-6), 4.62 (s, 1H, *H*-1″), 5.59 (s, 1H, *H*-2), 7.19 (d, J = 6.8 Hz, 2H, *H*–Ph), 7.23–7.43 (m, 5H, *H*–Ph), 7.52 (dd, J = 7.2, 2.0 Hz, 2H, *H*–Ph), 7.97 (d, J = 1.2 Hz, 1H, *H*-1′).

4.4. Reaction of D-erythrosylbenzylimine 5a–d with 1-(*tert*-butyldimethylsilyloxy)-1-methoxyethene

4.4.1. General procedure. The imine reaction mixture obtained in the precedent step (0.34–0.67 mmol) was refrigerated at −84 °C for 15 min, and $BF_3{\cdot}OEt_2$ (42–83 μL; 47–95 mg; 0.34–0.67 mmol) was added under magnetic stirring followed by 1-(*tert*-butyldimethylsilyloxy)-1-methoxyethene (79–150 μL; 63–130 mg; 0.34–0.67 mmol). The mixture was kept stirring under the conditions described for 1–2 h, and then allowed to recover at room temperature. The reaction mixture was passed through a pad of Celite®, and the filtrate was evaporated in the rotary evaporator to give a brownish oil, which was re-dissolved in chloroform (40 mL) and successively washed with water (3 × 20 mL), aqueous sat. $NaHCO_3$ (3 × 20 mL) followed by saturated NaCl solution (2 × 20 mL). The organic layers were combined and dried with anhydrous magnesium sulfate, filtered, and the solvent was evaporated to give a yellow oil residue. The crude product was subjected to column chromatography (silica, petroleum ether : ethyl acetate).

4.4.2. Synthesis of (*R*)-methyl-3-(benzylamino)-3-((2*R*,4*S*,5*R*)-5-hydroxy-2-phenyl-1,3-dioxan-4-yl)propanoate (6a). Imine **5a** (100 mg, 0.34 mmol) obtained previously; THF (4 mL); $BF_3{\cdot}OEt_2$ (42 μL; 47 mg; 0.34 mmol); 1-(*tert*-butyldimethylsilyloxy)-1-methoxyethene (79 μL; 63 mg; 0.34 mmol); 2 h. Product: yellow oil (112 mg; 0.30 mmol) η = 88%.[a]

Published on 08 November 2019. Downloaded by University of Texas Libraries on 1/4/2020 5:05:00 AM.

$[\alpha]_D^{17} = -13.3$ (*c* 0.6, MeOH); IR ν_{max} 3323, 1724 cm^{-1}; ^1H NMR (400 MHz, $CDCl_3$) δ 2.57 (dd, *J* = 16.4, 10.4 Hz, 1H, *H*-2′), 2.94 (dd, *J* = 16.4, 3.2 Hz, 1H, *H*-2′), 3.55 (ddd, *J* = 10.4, 4.4, 3.2 Hz, 1H, *H*-1′), 3.65 (s, 3H, OMe), 3.65 (t, *J* = 10.8 Hz, 1H, *H*-6), 3.90 (d, *J* = 12.4 Hz, 1H, *H*-1″), 3.93 (dd, *J* = 9.6, 4.4 Hz, 1H, *H*-4), 4.00 (ddd, *J* = 10.4, 9.6, 5.2 Hz, 1H, *H*-5), 4.03 (d, *J* = 12.4 Hz, 1H, *H*-1″), 4.35 (dd, *J* = 10.8, 5.2 Hz, 1H, *H*-6), 5.54 (s, 1H, *H*-2), 7.30–7.48 (m, 10H, *H*–Ph) ppm; ^{13}C NMR (100 MHz, $CDCl_3$) δ 33.9 (C-2′), 51.9 (OMe), 52.6 (C-1″), 56.4 (C-1′), 63.0 (C-5), 70.9 (C-6), 77.9 (C-4), 101.6 (C-2), 126.1, 127.7, 128.2, 128.5, 128.7, 129.1 (CH–Ph), 137.5, 138.4 (C-q), 172.8 (C═O) ppm; HRMS (ESI): calcd for $[C_{21}H_{26}NO_5^+]$: 372.1766 (M + H^+); found: 372.1803.

(a) A small fraction enriched in product **7a** (3 mg) was obtained from the chromatographic purification of compound **6a**.

Compound **7a**: ^1H NMR (400 MHz, $CDCl_3$) δ 2.61 (dd, *J* = 18.0, 7.6 Hz, 1H, *H*-7), 3.12 (dd, *J* = 18.0, 7.6 Hz, 1H, *H*-7), 3.38 (dt, *J* = 8.8, 7.6 Hz, 1H, *H*-8), 3.77 (t, *J* = 9.2 Hz, 1H, *H*-4), 3.77 (d, *J* = 13.2 Hz, 1H, CH_2–Ph), 3.83 (t, *J* = 10.4 Hz, 1H, *H*-6), 3.87 (d, *J* = 13.2 Hz, 1H, CH_2–Ph), 4.21 (ddd, *J* = 10.0, 9.6, 5.2 Hz, 1H, *H*-5), 4.45 (dd, *J* = 10.4, 4.8 Hz, 1H, *H*-6), 5.60 (s, 1H, *H*-2), 7.28–7.49 (m, 10H, *H*–Ph) ppm; ^{13}C NMR (100 MHz, $CDCl_3$) δ 36.2 (C-2′), 50.9 (C-7), 53.7 (C-8), 68.3 (C-6), 69.3 (C-5), 79.8 (C-4), 101.9 (C-2), 126.1, 127.3, 128.1, 128.4, 128.6, 129.4 (CH–Ph), 136.6, 139.3 (C-q), 168.4 (C═O) ppm.

4.4.3. Synthesis of (*R*)-methyl 3-((benzo[*d*][1,3]dioxol-4-ylmethyl)amino)-3-((2*R*,4*R*,5*R*)-5-hydroxy-2-phenyl-1,3-dioxan-4-yl)propanoate (6b). Imine **5b** (171 mg; 0.50 mmol); 1-(*tert*-butyldimethylsilyloxy)-1-methoxyethene (110 μL, 95 mg, 0.50 mmol); $BF_3{\cdot}OE_{t2}$ (62 μL, 71 mg, 0.50 mmol). Product: yellow oil (150 mg, 0.36 mmol); η = 72%; $[\alpha]_D^{24} = -16.0$ (*c* 0.9, DCM); IR (nujol) ν_{max} 3330, 1731 cm^{-1}; ^1H NMR (400 MHz, $CDCl_3$) δ 2.56 (dd, *J* = 16.4, 10.4 Hz, 1H, *H*-2′), 2.93 (dd, *J* = 16.0, 3.2 Hz, 1H, *H*-2′), 3.52 (dt, *J* = 10.4, 3.6 Hz, 1H, *H*-1′), 3.65 (dd, *J* = 10.4, 9.5 Hz, 1H, *H*-6), 3.66 (s, 3H, OMe), 3.79 (d, *J* = 12 Hz, 1H, *H*-1″), 3.93 (dd, *J* = 9.2, 4.0 Hz, 1H, *H*-4), 3.94 (d, *J* = 12.4 Hz, 1H, *H*-1″), 3.99 (ddd, *J* = 9.2, 5.2, 4.8 Hz, 1H, *H*-5), 4.33 (dd, *J* = 10.8, 5.2 Hz, 1H, *H*-6), 5.53 (s, 1H, *H*-2), 5.94 (d, *J* = 2 Hz, 2H, *H*-8″), 6.75–6.83 (m, 3H, *H*–Ph), 7.27–7.41 (m, 5H, *H*–Ph); ^{13}C NMR (100 MHz, $CDCl_3$) δ 33.9 (C-2′), 51.9 (OMe), 52.3 (C-1″), 56.7 (C-1′), 63.1 (C-5), 70.9 (C-6), 77.9 (C-4), 101.0 (C-8″), 101.6 (C-2), 108.3, 108.8, 121.7 (C-, C-4″, C-7″), 126.1, 126.2, 128.2, 128.4. 129.1 (CH–Ph), 132.3 (C-2″), 137.5 (C-q), 147.1 (C-q), 147.9 (C-q), 172.8 (C═O). Elemental analysis, calcd for $C_{22}H_{25}NO_7$: C, 63.6; H, 6.07; N, 3.37. Found C, 63.2; H, 6.10; N, 3.10.

4.4.4. Synthesis of (*R*)-methyl 3-((4-fluorobenzyl)amino)-3-((2*R*,4*R*,5*R*)-5-hydroxy-2-phenyl-1,3-dioxan-4-yl)propanoate (6c). Imine **5c** (158 mg; 0.50 mmol); 1-(*tert*-butyldimethylsilyloxy)-1-methoxyethene (110 μL, 95 mg, 0.50 mmol), $BF_3{\cdot}OEt_2$ (62 μL, 71 mg, 0.50 mmol). Product: yellow oil (96 mg, 0.25 mmol); η = 50%; $[\alpha]_D^{24} = -27.0$ (*c* 0.6, DCM); IR (nujol) ν_{max} 3331, 1732 cm^{-1}; ^1H NMR (400 MHz, $CDCl_3$) δ 2.67 (dd, *J* = 16.0, 9.2 Hz, 1H, *H*-2′), 2.95 (dd, *J* = 16.8, 4.1 Hz, 1H, *H*-2′), 3.60 (dt, *J* = 9.6, 4.0 Hz, 1H, *H*-1′), 3.64 (dd, *J* = 10.8, 9.6 Hz, 1H, *H*-6), 3.66 (s, 3H, OMe), 3.93 (d, *J* = 13.2 Hz, 1H, *H*-1″), 3.94 (dd, *J* = 9.2, 3.6 Hz, 1H, *H*-4), 4.00 (ddd, *J* = 10.4, 9.2, 4.8 Hz, 1H, *H*-5), 4.03 (d, *J* = 12.8 Hz, 1H, *H*-1″), 4.33 (dd, *J* = 10.8, 5.2 Hz, 1H, *H*-6), 5.51 (s, 1H, *H*-2), 7.01–7.06 (m, 2H, *H*–Ph), 7.27–7.47 (m, 7H, *H*–Ph) ppm; ^{13}C NMR (100 MHz, $CDCl_3$) δ 33.4 (C-2′), 51.3 (OMe), 52.0 (C-1″), 53.7 (C-1′), 62.7 (C-5), 70.9 (C-6), 78.3 (C-4), 101.6 (C-2), 115.4 (d, *J* = 21 Hz, C-4″ or C-6″), 115.7 (d, *J* = 21 Hz, C-4″ or C-6″), 126.1, 128.3, 128.4, 129.1, 129.5 (CH–Ph), 129.8 (d, *J* = 8.0 Hz, C-3″ or C-7″), 130.5 (d, *J* = 8.0 Hz, C-3″ or C-7″), 132.7, 137.3 (C-q), 162.5 (d, *J* = 246 Hz, C-5″), 172.5 (C═O). HRMS (ESI): calcd for $C_{21}H_{26}FNO_5$: 390.1717 (M + H^+); found: 390.1717.

4.4.5. Synthesis of (*R*)-methyl 3-((4-chlorobenzyl)amino)-3-((2*R*,4*R*,5*R*)-5-hydroxy-2-phenyl-1,3-dioxan-4-yl)propanoate (6d). Imine **5d** (222 mg; 0.67 mmol); 1-(*tert*-butyldimethylsilyloxy)-1-methoxyethene (150 μL, 130 mg; 0.67 mmol); $BF_3{\cdot}OEt_2$ (83 μL, 95 mg, 0.67 mol). Product: yellow oil (280 mg, 0.67 mmol); η = quant. $[\alpha]_D^{24} = -42$ (*c* 0.6, DCM); IR (nujol) ν_{max} 3327, 1728 cm^{-1}; ^1H NMR (400 MHz, $CDCl_3$) δ 2.57 (dd, *J* = 16.4, 10.0 Hz, 1H, *H*-2′), 2.93 (dd, *J* = 16.0, 3.2 Hz, 1H, *H*-2′), 3.50 (dt, *J* = 10.0, 3.6 Hz, 1H, *H*-1′), 3.64 (dd, *J* = 10.4, 9.6 Hz, 1H, *H*-6), 3.65 (s, 3H, OMe), 3.87 (d, *J* = 12.4 Hz, 1H, *H*-1″), 3.91 (dd, *J* = 10.0, 4.0 Hz, 1H, *H*-4), 3.98 (d, *J* = 12.8 Hz, 1H, *H*-1″), 3.99 (ddd, *J* = 9.6, 5.2, 4.4 Hz, 1H, *H*-5), 4.33 (dd, *J* = 10.8, 5.2 Hz, 1H, *H*-6), 5.53 (s, 1H, *H*-2), 7.26–7.39 (m, 7H, H–Ph), 7.45–7.48 (m, 2H, H–Ph); ^{13}C NMR (100 MHz, $CDCl_3$) δ 33.9 (C-2′), 51.8 (OMe), 51.9 (C-1″), 56.8 (C-1′), 63.1 (C-5), 70.9 (C-6), 78.0 (C-4), 101.6 (C-2), 126.1, 128.3, 128.8, 129.1, 129.7 (CH–Ph), 133.4 (C-q), 136.9 (C-q), 137.4 (C-q) 172.8 (C═O). HRMS (ESI): calcd for $C_{21}H_{26}ClNO_5$: 406.1421/408.1392 (M + H^+); found: 406.1420/408.1392.

5. Treatment of the adducts 6a–d with acids

5.1. Hydrochloric acid

5.1.1. General procedure. (i) To a solution of the β-aminoester **6a–d** (60–111 mg; 0.15–0.27 mmol) in dioxane (2–4 mL) was added hydrochloric acid 37% (1.5–2.8 mL) to form a 6 M solution. The reaction mixture was stirred for 2 h at room temperature, evaporated in the rotary evaporator until a solid foam or a brown oil was formed (a mixture of compounds **13** and **8** in a 2 : 1 ratio). The reaction mixture was used in the next stage.

(ii) To the reaction mixture obtained in (i) (60–111 mg, 0.15–0.27 mmol) was added water (2.5–3.3 mL) and solid KOH (23–33 mg, 0.14–0.20 mmol). The reaction mixture was stirred overnight. An aqueous suspension of acid resin IR-120 (H^+) was added until pH 7, and kept under hand stirring. The resin was filtered off, and the solvent was removed in the rotary evaporator to give a pasty residue. This was dissolved in ethanol (2 mL), filtered and evaporated to give light brownish oils (20–70 mg, 0.074–0.26 mmol, 48–96.3% yield), as the respective L-homoprolines **8a–d**.

5.1.2. Synthesis of 2-((2*S*,3*S*,4*R*)-*N*-benzyl-3,4-dihydroxypyrrolidin-2-yl)acetic acid (8a). (i) β-Aminoester **6a** (100 mg, 0.27 mmol); 1,4-dioxane (3 mL); HCl 37% (2.5 mL). Quantitative mixture of compounds **13a : 8a** in a 2 : 1 ratio, by ^1H NMR.

 This journal is © The Royal Society of Chemistry 2019

Published on 08 November 2019. Downloaded by University of Texas Libraries on 1/4/2020 5:05:00 AM.

Compound **13a**[(a)]: ^{1}H NMR (400 MHz, D_2O) δ 3.10 (dd, J = 19.2, 2.0 Hz, 1H, *H*-3), 3.30 (dd, J = 19.2, 8.4 Hz, 1H, *H*-3), 3.78 (dd, J = 12.4, 2.0 Hz, 1H, *H*-7), 3.90 (dd, J = 12.4, 3.6 Hz, 1H, *H*-7), 4.17 (d, J = 13.2 Hz, 1H, *H*-1′), 4.32–4.36 (m, 2H, *H*-3a + *H*-6), 4.44 (d, J = 13.2 Hz, 1H, *H*-1′), 4.87 (dd J = 5.6, 4.4 Hz, 1H, *H*-6a), 7.44–7.51 (m, 10H, *H*–Ph) ppm; ^{13}C NMR (100 MHz, D_2O) δ 31.5 (C-3), 49.2 (C-1′), 55.6 (C-3a), 61.1 (C-7), 68.1 (C-6), 80.8 (C-6a), 128.9 (C-2), 129.0 (C-3′ or C-4′ or C-5′), 129.3 (C-3′ or C-4′ or C-5′), 129.5 (C-3′ or C-4′ or C-5′), 175.3 (C═O) ppm.

(a) The ^{1}H NMR and ^{13}C NMR descriptions were taken from the crude material of the reaction of compound **6a** with TFA, where a 3 : 1 ratio of compounds **13a** (3) : **8a** (1) was isolated.

(ii) To the mixture obtained in step (i) (72.6 mg) was added water (3.0 mL) and solid KOH (30 mg, 0.18 mmol). Product **8a**: (70 mg, 0.26 mmol); η = 96.3%; $[\alpha]_D^{24}$ = −20.5 (c 0.4, MeOH); IR (nujol) ν_{max} 3187, 1680 cm^{-1}; ^{1}H NMR (400 MHz, D_2O) δ 2.89 (dd, J = 18.0, 6.0 Hz, 1H, CH_2CO$_2$H), 3.95 (dd, J = 18.0, 6.4 Hz, 1H, CH_2CO$_2$H), 3.51 (dd, J = 12.0, 6.4 Hz, 1H, *H*-5), 3.65 (dd, J = 12.0, 4.0 Hz, 1H, *H*-5), 3.80 (td, J = 6.8, 3.2 Hz, 1H, *H*-2), 3.86 (td, J = 5.6, 4.0 Hz, 1H, *H*-4), 3.91 (dd, J = 5.6, 3.2 Hz, 1H, *H*-3), 4.32 (d, J = 13.2 Hz, 1H, *H*-1′), 4.46 (d, J = 13.2 Hz, 1H, *H*-1′), 7.54 (s, 5H, *H*–Ph) ppm; ^{13}C NMR (100 MHz, D_2O) δ 30.2 (*C*H$_2$CO$_2$H), 46.4 (C-1′), 52.9 (C-2), 59.3 (C-5), 66.0 (C-3), 70.3 (C-4), 126.6 (C-3′ or C-4′ or C-5′), 127.1 (C-3′ or C-4′ or C-5′), 127.2 (C-3′ or C-4′ or C-5′), 127.8 (C-2′), 172.2 (C═O) ppm; elemental analysis, calcd for $C_{13}H_{17}NO_4$: C, 62.14; H, 6.82; N, 5.57. Found C, 62.20; H, 6.65; N, 5.76.

5.1.3. Synthesis of 2-((2*S*,3*S*,4*R*)-*N*-piperonyl-3,4-dihydroxypyrrolidin-2-yl)acetic acid (8b). (i) β-Aminoester **6b** (100 mg, 0.24 mmol); 1,4-dioxane (3 mL); HCl 37% (2.5 mL). A quantitative mixture of compounds **13b** : **8b** in a 2 : 1 ratio.

Compound **13b** was identified by ^{1}H NMR (400 MHz, D_2O) δ 3.00 (dd, J = 18.8, 1.6 Hz, 1H, *H*-3), 3.23 (dd, J = 18.8, 8.0 Hz, 1H, *H*-3), 3.72 (dd, J = 12.4, 2.0 Hz, 1H, *H*-7), 3.84 (dd, J = 12.0, 3.2 Hz, 1H, *H*-7), 4.03 (d, J = 13.2 Hz, 1H, *H*-1′), 4.14 (d, J = 13.6 Hz, 1H, *H*-1′), 4.25–4.31 (m, 2H, *H*-3a + *H*-6), 4.67 (dd, J = 5.6 Hz, 4.8 Hz, 1H, *H*-6a), 5.95 (s, 2H, *H*-8′)[(a)], 6.88–6.94 (m, 3H, *H*–Ph)[(a)].

(a) These signals are coincident in the ^{1}H NMR spectrum of the mixture of the two compounds **13b** and **8b**.

(ii) To a mixture obtained in step (i) (78 mg) was added water (3.0 mL) and solid KOH (30 mg, 0.18 mmol). Product **8b**: (56 mg, 0.19 mmol); η = 79%; $[\alpha]_D^{24}$ = −25.0 (c 0.6, MeOH); IR (nujol) ν_{max} 3350, 1586 cm^{-1}; ^{1}H NMR (400 MHz, D_2O) δ 2.40–2.70 (m, 2H, CH_2CO$_2$H), 3.47–3.58 (m, 2H, *H*-4 + *H*-5), 3.68 (br d, J = 12.0 Hz, 1H, *H*-5), 3.82 (br s, 2H, *H*-3 + *H*-4), 4.12 (d, J = 13.2 Hz, 1H, *H*-1′), 4.24 (d, J = 13.2 Hz, 1H, *H*-1′), 5.93 (s, 1H, *H*-8′), 5.94 (s, 1H, *H*-8′), 6.85–6.94 (m, 3H, *H*–Ph); ^{13}C NMR (100 MHz, D_2O) δ 35.5 (*C*H$_2$CO$_2$H), 48.8 (C-1′), 55.5 (C-2), 61.7 (C-5), 69.6 (C-3), 72.7 (C-4), 100.9 (C-8′), 108.3, 109.1, 122.9 (CH–Ph), 127.2, 146.9, 147.1 (C-q), 178.1 (C═O). HRMS (ESI): calcd for $C_{14}H_{20}NO_7$: 314.1234 (M + H_2O + H^+); found: 314.1233.

5.1.4. Synthesis of 2-((2*S*,3*S*,4*R*)-*N*-(4-fluorobenzyl)-3,4-dihydroxypyrrolidin-2-yl)acetic acid (8c). (i) β-Aminoester **6c** (60 mg, 0.15 mmol); solvent: 1,4-dioxane (2 mL); HCl 37% (1.5 mL). A quantitative mixture of compounds **13c** : **8c** in a 2 : 1 ratio. Compound **13c** was identified by ^{1}H NMR (400 MHz, D_2O) δ 2.91 (dd, J = 19.2, 2.0 Hz, 1H, *H*-3), 3.12 (dd, J = 19.2, 8.0 Hz, 1H, *H*-3), 3.59 (dd, J = 12.4, 2.0 Hz, 1H, *H*-7), 3.70 (dd, J = 12.4, 3.2 Hz, 1H, *H*-7), 3.99 (d, J = 13.6 Hz, 1H, *H*-1′), 4.10 (d, J = 13.2 Hz, 1H, *H*-1′), 4.23–4.27 (m, 2H, *H*-3a + *H*-6), 4.77 (dd, J = 6.0, 4.4 Hz, 1H, *H*-6a), 7.01–7.05 (t, 2H, *H*-4′ + *H*-6′), 7.28–7.31 (m, 2H, *H*-3′ + *H*-7′).

(ii) To a mixture obtained in step (i) (43 mg) was added water (2.5 mL) and solid KOH (23 mg, 0.14 mmol). Product **8c**: (20 mg, 0.074 mmol); η = 48%; $[\alpha]_D^{24}$ = −23.0 (c 0.6, MeOH); IR (nujol) ν_{max} 3347, 2926, 2856, 1660 cm^{-1}; ^{1}H NMR (400 MHz, D_2O) δ 2.55 (dd, J = 14.8 Hz, 6.8 Hz, 1H, CH_2CO$_2$H), 2.60 (dd, J = 14.8 Hz, 6.4 Hz, 1H, CH_2CO$_2$H), 3.27 (td, J = 6.8 Hz, 2.8 Hz, 1H, *H*-2), 3.50 (dd, J = 12.0 Hz, 6.0 Hz, 1H, *H*-5), 3.67 (dd, J = 12.0 Hz, 4.8 Hz, 1H, *H*-5), 3.73 (dd, J = 6.0, 2.8 Hz, 1H, *H*-3), 3.76–3.80 (m, 1H, *H*-4), 3.79 (d, J = 12.8 Hz, 1H, *H*-1′), 3.96 (d, J = 13.2 Hz, 1H, *H*-1′), 7.13–7.18 (m, 2H, *H*–Ph), 7.39–7.43 (m, 2H, *H*–Ph); ^{13}C NMR (100 MHz, D_2O) δ 38.5 (*C*H$_2$CO$_2$H), 49.5 (C-1′), 55.7 (C-2), 62.3 (C-5), 71.5 (C-3), 73.4 (C-4), 115.2 (d, J = 22.0 Hz, C-4′ or C-6′), 115.4 (d, J = 22.0 Hz, C-4′ or C-6′), 130.5 (d, J = 8.0 Hz, C-3′ or C-7′), 130.6 (d, J = 8.0 Hz, C-3′ or C-7′), 134.2 (C-2′), 161.9 (d, J = 241.0 Hz, C-5′), 180.3 (C═O). HRMS (ESI): calcd for $C_{13}H_{19}FNO_5$: 288.1242 (M + H_2O + H^+); found: 288.1242.

5.1.5. Synthesis 2-((2*S*,3*S*,4*R*)-*N*-(4-chlorobenzyl)-3,4-dihydroxypyrrolidin-2-yl)acetic acid (8d). (i) β-Aminoester **6d** (111 mg, 0.27 mmol); solvent: 1,4-dioxane (4 mL); HCl 37% (2.8 mL). A quantitative mixture of compounds **13d** : **8d** in a 2 : 1 ratio. Compound **13d** was identified by ^{1}H NMR (400 MHz, D_2O) δ 3.02 (dd, J = 19.2, 2.0 Hz, 1H, *H*-3), 3.23 (dd, J = 19.2, 8 Hz, 1H, *H*-3), 3.70 (dd, J = 12.4, 2.0 Hz, 1H, *H*-7), 3.83 (dd, J = 12.4, 3.6 Hz, 1H, *H*-7), 4.09 (d, J = 13.2 Hz, 1H, *H*-1′), 4.22–4.29 (m, 2H, *H*-3a + *H*-6), 4.35 (d, J = 13.2 Hz, 1H, *H*-1′), 4.80 (dd, J = 6.0, 4.8 Hz, 1H, *H*-6a), 7.34–7.45 (m, 4H, *H*–Ph).

(ii) To the mixture obtained in step (i) (83 mg) in water (3.3 mL) was added solid KOH (33 mg, 0.20 mmol). Product **8d**: (66 mg; 0.23 mmol); η = 85.0%; $[\alpha]_D^{24}$ = + 6.0 (c 0.7, MeOH); IR (nujol) ν_{max} 3346, 1690 cm^{-1}; ^{1}H NMR (400 MHz, D_2O) δ 2.64 (dd, J = 16.4 Hz, 6.8 Hz, 1H, CH_2CO$_2$H), 2.70 (dd, J = 16.4 Hz, 6.4 Hz, 1H, CH$_2$CO$_2$H), 3.52 (dd, J = 11.6 Hz, 5.6 Hz, 1H, *H*-5), 3.60 (td, J = 6.4 Hz, 3.2 Hz, 1H, *H*-2), 3.67 (dd, J = 12.8 Hz, 4.4 Hz, 1H, *H*-5), 3.80–3.87 (m, 2H, *H*-3 + *H*-4), 4.16 (d, J = 13.2 Hz, 1H, *H*-1′), 4.28 (d, J = 13.2 Hz, 1H, *H*-1′), 7.44 (d, J = 8.4 Hz, 2H, *H*–Ph), 7.48 (d, J = 8.4 Hz, 2H, *H*–Ph); ^{13}C NMR (100 MHz, D_2O) δ 34.4 (CH$_2$CO$_2$H), 47.8 (C-1′), 55.9 (C-2), 61.6 (C-5), 69.1 (C-3), 72.6 (C-4), 128.7, 130.7 (CH–Ph), 130.5, 134.1 (C-q), 177.4 (C═O). HRMS (ESI): calcd for $C_{13}H_{17}ClNO_4$: 286.0846 (M + H^+); found: 286.0851.

5.2. Trifluoroacetic acid

5.2.1. Formation of a mixture of salts of trifluoroacetic acid: (3a*R*,6*R*,6a*S*)-4-benzyl-6-hydroxyhexahydro-2*H*-furo[3,2-*b*]pyrrol-2-one (13a) and 2-((2*R*,3*S*,4*R*)-1-benzyl-3,4-dihydroxypyrrolidin-2-yl) acetic acid (8a). To a solution of β-aminoester **6a** (30 mg; 0.08 mmol) in 1,4-dioxane (1.62 mL) was added trifluoroacetic acid until a 6 M acid solution was formed

Published on 08 November 2019. Downloaded by University of Texas Libraries on 1/4/2020 5:05:00 AM.

(1.38 mL). The reaction mixture was run at room temperature, under magnetic stirring for one week. The solvents were removed in the rotary evaporator, leaving a brownish oil consisting of a virtually pure mixture of compounds **13a** and **8a**, in a 3 : 1 ratio and quantitative yield.

5.3. Bromic acid in acetic acid

5.3.1. Formation of a mixture of salts of hydrobromic acid: (3a*R*,6*R*,6a*S*)-4-benzyl-6-hydroxyhexahydro-2*H*-furo[3,2-*b*]pyrrol-2-one (13a) and 2-((2*R*,3*S*,4*R*)-1-benzyl-3,4-dihydroxypyrrolidin-2-yl) acetic acid (8a). A solution of β-aminoester **6a** (50 mg; 0.13 mmol) in 33% bromic acid in acetic acid (1 mL) was stirred at room temperature for 2 hours. Then methanol (3.6 mL) was added, and the reaction mixture was kept under magnetic stirring for three days. The solvents were removed in the rotary evaporator, leaving a brownish oil consisting of a virtually pure mixture of compounds **13a** and **8a**, in a 1 : 1 ratio and quantitative yield.

6. Cleavage of the benzyl group in compound 8a to give 8e

To the benzylated L-homoproline (**8a**) (20 mg, 0.075 mmol) in MeOH (4 mL) in the presence of a catalyst (Pd/C 10 mol%) was added 1,1,2-trichloroethane (8 μL, 1.1 equiv.). The mixture was stirred for 2 days under a hydrogen atmosphere (1 atm). The mixture was filtered through a glass-fiber filter. To the filtrate was added 0.01 M aq. solution of KOH until pH = 12. The solvent was removed in the rotary evaporator to give an yellow oil, compound **8e** (12 mg, 0.061 mmol); η = 81%; $[\alpha]_D^{21}$ = −32.3 (*c* 0.01, MeOH); IR (nujol) ν_{max} 3328, 3257, 1722 cm^{-1}; ^1H NMR (400 MHz, D_2O) δ 2.41 (dd, *J* = 7.6 Hz, 15.2 Hz, 1H, CH_2CO_2H)[a], 2.58 (dd, *J* = 5.2 Hz, 14.8 Hz, 1H, CH_2CO_2H), 3.23 (q, *J* = 5.2 Hz, 1H, *H*-2), 3.63–3.68 (m, 1H, *H*-4), 3.23 (t, *J* = 4.8 Hz, 1H, *H*-3), 3.76–3.84 (m, 2H, *H*-5) ppm; ^{13}C NMR (100 MHz, D_2O) δ 32.2(CH_2CO_2H), 61.8 (C-2), 62.4 (C-5), 71.5 (C-3), 72.6 (C-4), 179.2 (C=O) ppm;* HRMS (ESI), calcd for $C_6H_{12}NO_4$: 162.0761 ($M + H^+$); found: 162.0758.

(a) Contaminated with DMSO.

7. Computational calculations (methodology)

All geometry optimizations were performed with Gaussian 09 [22] by applying density functional theory[23] with the B3LYP functional[24–28] together with the 6-31G(d) basis set,[29–32] with a fine integration grid.

In all geometry optimizations, we first searched for the transition state starting from a structure like the reactant model. This was generally obtained with unidimensional scans along the particular reaction coordinate in which we were interested. Once a putative transition structure was located, it was fully optimized and characterized. Subsequently, the reactants and products associated with the calculated transition state structures were determined through intrinsic reaction coordinate (IRC) calculations that were followed by a final geometry optimization.[33] In all cases, the geometry optimizations and the stationary points were obtained with standard Gaussian convergence criteria. The transition-state structures, reactants and products were all verified by vibrational frequency calculations. All the TS structures have only one imaginary frequency with the correct transition vector, whereas the reactants and products have all the frequencies positive.

The free final energies were calculated with density functional theory, as a sum of the electronic energies, using the all-electron 6-311++G(3df,2pd) basis set and the functional M062X, plus the ZPE, thermal, and entropic energies (T = 310.15 K, P = 1 bar), calculated with the B3LYP functional but with the 6-31G(d) basis set and the dispersion corrections with the DFT-D3 methodology.[34,35] This value was also added to the contribution of a conductor-like polarizable continuum model using the integral equation formalism variant (IEF-PCM),[36–38] as implemented in Gaussian 09, to simulate the different solvents employed in the experimental work. To this end, different dielectric constants were applied: water, 78.355; acetic acid, 6.253 and 1,4-dioxane, 2.210.

All the activation and reaction energies provided in the text and figures refer to free energy differences calculated at the M06DX/6-311++G(3df,2pd) level of theory.

8. Conclusion

The study describes the development of a very simple, high yielding strategy for the synthesis of (3*S*,4*R*)-dihydroxy L-homoprolines from D-erythrose. Trivial reagents, cascade reactions, no purification needs, and completely selective reactions make this process highly appealing for the synthesis of (3*S*,4*R*)-dihydroxy homoprolines of L-stereochemistry. Considering the biological importance of the final products, as new molecular scaffolds of an important type, conjugated with the simplicity of the chemical process, an insight on the energetics of reactions involved became a major demand. As the cyclization mechanism of 6-carbon atom D-erythrosyl derivatives to a related type of 1,4-lactone intermediate had been previously studied, the theoretical work was now focused on the transformation of these intermediates into (3*S*,4*R*)-dihydroxy L-homoprolines.

The computational results reveal that the mechanism of the formation of the *N*-benzyl-(3*S*,4*R*)-dihydroxy L-homoprolines **8a** from 1,4-lactones **12a** diverges under acidic or basic conditions, although they share some similarities. In both, acid and basis cases, the catalysts favor the proton shuttle that is required for the cleavage of the lactones. The main difference in the mechanism is that with KOH a zwitterionic reaction intermediate in which K^+ takes part is involved. This effect favors the intramolecular hydrogen bond network between the compound and the two water molecules required for the next step. This effect is not observed in acid catalysis, which leads to a significant increase in the calculated activation free energies.

 This journal is © The Royal Society of Chemistry 2019

Published on 08 November 2019. Downloaded by University of Texas Libraries on 1/4/2020 5:05:00 AM.

Conflicts of interest

There are no conflcts of interest to declare.

Acknowledgements

We thank the NMR Portuguese network (PTNMR, Bruker Avance III 400-Univ. Minho), and FCT and FEDER (European Fund for Regional Development)-COMPETE-QREN-EU for financial support to CQ/UM. We also thank Search-ON2 for the revitalization of the HPC infrastructure of UMinho, (NORTE-07-0162-FEDER-000086), co-funded by the North Portugal Regional Operational Programme (ON.2-O Novo Norte), under the National Strategic Reference Framework (NSRF), through the European Regional Development Fund (ERDF) and the doctoral scholarship SFRH/BD/87292/2012.

References

1 S. Hannessian, *Total Synthesis of Natural Products: The Chiron Approach*, Pergamon, Oxford, 1983.
2 M. Miyashita, N. Chida and A. Yoshikoshi, *J. Chem. Soc., Chem. Commun.*, 1984, 195.
3 R. C. Bernotas and B. Ganem, *Tetrahedron Lett.*, 1985, **26**, 4981.
4 (*a*) F. Zanardi, L. Battistini, M. Nespi, G. Rassu, P. Spanu, M. Cornia and G. Casiraghi, *Tetrahedron: Asymmetry*, 1996, **7**(4), 1167–1180; (*b*) M. Fujii, T. Miura, T. Kajimoto and Y. Ida, *Synlett*, 2000, 1046; C. M. Taylor, C. E. Jones and K. Bopp, *Tetrahedron*, 2005, **61**, 9611–9617.
5 (*a*) T. Nakajima and B. E. Volcani, *Science*, 1969, **164**, 1400–1401; (*b*) I. L. Karle, J. W. Daly and B. Witkop, *Science*, 1969, **164**, 1401–1402; (*c*) I. L. Karle, *Acta Crystallogr., Sect. B: Struct. Crystallogr. Cryst. Chem.*, 1970, **26**, 765–770.
6 A. Buku, H. Faulstich, T. Wieland and J. Dabrowski, *Proc. Natl. Acad. Sci. U. S. A.*, 1980, **77**, 2370–2371.
7 H. Faulstich, A. Buku, H. Bodenmueller and T. Wieland, *Biochemistry*, 1980, **19**, 3334–3343.
8 K. Csatayov, S. G. Davies, A. L. A. Figuccia, A. M. Fletcher, J. G. Ford, J. A. Lee, P. M. Roberts, B. G. Saward, H. Song and J. E. Thomson, *Tetrahedron*, 2015, **71**, 9131–9142; S. G. Davies, E. M. Foster, J. A. Lee, P. M. Roberts and J. E. Thomson, *Tetrahedron*, 2013, **69**, 8680.
9 D. S. Freitas, J. Noro, A. Drogalin, M. C. S. Fernandes, A. V. M. Baptista, J. F. C. Parente, J. E. Rodríguez-Borges, A. Gil Fortes and M. J. Alves, *Synthesis*, 2019, 2720–2272.
10 E. Vass, M. Hollósi, F. Besson and R. Buchet, *Chem. Rev.*, 2003, **103**, 1917–1954.
11 J. A. Smith and L. G. Pease, *Crit. Rev. Biochem.*, 1980, **8**, 315–399.
12 L. M. Gierasch, C. M. Deber, V. Madison, C. H. Niu and E. R. Blout, *Biochemistry*, 1981, **20**, 4730–4738.
13 G. D. Rose, L. M. Gierasch and J. A. Smith, *Adv. Protein Chem.*, 1985, **37**, 1–109.
14 I. D. Kuntz, *J. Am. Chem. Soc.*, 1972, **94**, 4009–4012.
15 F. Sussman, V. M. Sánchez-Pedregal, J. C. Estévez, R. Balo, J. Jiménez-Barbero, A. Ardá, A. Gimeno, M. Royo, M. C. Villaverde and R. J. Estévez, *Chem. – Eur. J.*, 2018, **24**, 1–6.
16 Y. J. Chung, L. A. Christianson, H. E. Stanger, D. R. Powell and S. H. J. Gellman, *Am. Chem. Soc.*, 1998, **120**, 10555–10556.
17 F. Schumann, A. Müller, M. Koksch, G. Müller and N. Sewald, *J. Am. Chem. Soc.*, 2000, **122**, 12009–12010.
18 S. R. Baker, D. W. Clissold and A. McKillop, *Tetrahedron Lett.*, 1988, **29**, 991–994; P. Zimmermann and R. R. Schmidt, *Liebigs Ann. Chem.*, 1988, 663–667.
19 M. Fengler-Veith, O. Schwardt, U. Kautz, B. Krämer and V. Jäger, *Org. Synth.*, 2002, **78**, 123.
20 J. Ferreira, V. C. M. Duarte, J. Noro, A. Gil Fortes and M. J. Alves, *Org. Biomol. Chem.*, 2016, **14**, 2930–2937.
21 J. F. Rocha, D. S. Freitas, J. Noro, C. S. S Teixeira, C. E. A. Sousa, M. J. Alves and N. M. F. S. A. Cerqueira, *J. Org. Chem.*, 2018, **83**, 8011–8019.
22 M. J. Frisch, G. W. Trucks, H. B. Schlegel, G. E. Scuseria, M. A. Robb, J. R. Cheeseman, G. Scalmani, V. Barone, B. Mennucci, G. A. Petersson, H. Nakatsuji, M. Caricato, X. Li, H. P. Hratchian, A. F. Izmaylov, J. Bloino, G. Zheng, J. L. Sonnenberg, M. Hada, M. Ehara, K. Toyota, R. Fukuda, J. Hasegawa, M. Ishida, T. Nakajima, Y. Honda, O. Kitao, H. Nakai, T. Vreven, J. A. Montgomery Jr., J. E. Peralta, F. Ogliaro, M. J. Bearpark, J. Heyd, E. N. Brothers, K. N. Kudin, V. N. Staroverov, R. Kobayashi, J. Normand, K. Raghavachari, A. P. Rendell, J. C. Burant, S. S. Iyengar, J. Tomasi, M. Cossi, N. Rega, N. J. Millam, M. Klene, J. E. Knox, J. B. Cross, V. Bakken, C. Adamo, J. Jaramillo, R. Gomperts, R. E. Stratmann, O. Yazyev, A. J. Austin, R. Cammi, C. Pomelli, J. W. Ochterski, R. L. Martin, K. Morokuma, V. G. Zakrzewski, G. A. Voth, P. Salvador, J. J. Dannenberg, S. Dapprich, A. D. Daniels, Ö. Farkas, J. B. Foresman, J. V. Ortiz, J. Cioslowski and D. J. Fox, *Gaussian 09*, Gaussian, Inc, Wallingford, CT, USA, 2009.
23 P. Hohenberg and W. Kohn, Inhomogeneous Electron Gas, *Phys. Rev.*, 1964, **136**(3b), B864.
24 A. D. Becke, A new mixing of Hartree–Fock and local density-functional theories, *J. Chem. Phys.*, 1993, **98**(2), 1372–1377.
25 A. D. Becke, Density-functional thermochemistry. III. The role of exact exchange, *J. Chem. Phys.*, 1993, **98**(7), 5648–5652.
26 C. T. Lee, W. T. Yang and R. G. Parr, Development of the Colle-Salvetti correlation-energy formula into a functional of the electron density, *Phys. Rev. B: Condens. Matter Mater. Phys.*, 1988, **37**(2), 785–789.
27 S. H. Vosko, L. Wilk and M. Nusair, Accurate spin-dependent electron liquid correlation energies for local spin density calculations: a critical analysis, *Can. J. Phys.*, 1980, **58**(8), 1200–1211.
28 P. J. Stephens, F. J. Devlin, C. F. Chabalowski and M. J. Frisch, Ab Initio Calculation of Vibrational

Published on 08 November 2019. Downloaded by University of Texas Libraries on 1/4/2020 5:05:00 AM.

Absorption and Circular Dichroism Spectra Using Density Functional Force Fields, *J. Phys. Chem.*, 1994, **98**(45), 11623–11627.

29 V. A. Rassolov, M. A. Ratner, J. A. Pople, P. C. Redfern and L. Curtiss, 6-31G* basis set for third-row atoms, *J. Comput. Chem.*, 2001, **22**(9), 976–984.

30 R. Ditchfield, W. J. Hehre and J. A. Pople, Self-Consistent Molecular-Orbital Methods. IX. An Extended Gaussian-Type Basis for Molecular-Orbital Studies of Organic Molecules, *J. Chem. Phys.*, 1971, **54**(2), 724.

31 P. C. Hariharan and J. A. Pople, Accuracy of AH n equilibrium geometries by single determinant molecular orbital theory, *Mol. Phys.*, 1974, **27**(1), 209–214.

32 M. S. Gordon, The isomers of silacyclopropane, *Chem. Phys. Lett.*, 1980, **76**(1), 163–168.

33 N. Cerqueira, P. A. Fernandes and M. J. Ramos, Protocol for Computational Enzymatic Reactivity Based on Geometry Optimisation, *ChemPhysChem*, 2018, **19**(6), 669–689.

34 S. Grimme, J. Antony, S. Ehrlich and H. Krieg, A consistent and accurate ab initio parametrization of density functional dispersion correction (DFT-D) for the 94 elements H-Pu, *J. Chem. Phys.*, 2010, **132**(15), 154104.

35 S. Grimme, S. Ehrlich and L. Goerigk, Effect of the damping function in dispersion corrected density functional theory, *J. Comput. Chem.*, 2011, **32**(7), 1456–1465.

36 G. Scalmani and M. J. Frisch, Continuous surface charge polarizable continuum models of solvation. I. General formalism, *J. Chem. Phys.*, 2010, **132**(11), 114110.

37 E. Cances, B. Mennucci and J. Tomasi, A new integral equation formalism for the polarizable continuum model: Theoretical background and applications to isotropic and anisotropic dielectrics, *J. Chem. Phys.*, 1997, **107**(8), 3032–3041.

38 J. Tomasi, B. Mennucci and R. Cammi, Quantum mechanical continuum solvation models, *Chem. Rev.*, 2005, **105**(8), 2999–3093.

 This journal is © The Royal Society of Chemistry 2019